RSC Advances

PAPER

View Article Online
View Journal | View Issue



Cite this: *RSC Adv.*, 2018, **8**, 213

# Synthesis, magnetic and transport properties of HTP-$Ni_3Sn_2$ single crystals obtained by the chemical vapor transport method

Cong Xian *[ab] and Jian Wang[a]

Received 10th November 2017
Accepted 12th December 2017

DOI: 10.1039/c7ra12322a

rsc.li/rsc-advances

Here, we report the synthesis, magnetic properties and transport properties of HTP-$Ni_3Sn_2$ single crystals. The magnetic measurements reveal that HTP-$Ni_3Sn_2$ has a paramagnetic temperature dependence and the *c* axis has a stronger magnetic interaction. Despite the existence of strong antiferromagnetic interactions, the long range magnetic order is not observed due to the geometrical frustration. Moreover, the sublinear temperature dependence of the resistivity is presented, which is attributed to short-range correlations among the geometrical frustration. Our study suggests that the geometrical frustration has an important influence on the physical properties of HTP-$Ni_3Sn_2$.



## 1. Introduction

Frustrated materials are interesting because their physical properties are difficult to predict. And frustration can lead to qualitatively new states of matter and novel physical properties, such as quantum criticality,[1–3] quantum or topological anomalous Hall effect,[4–8] spin liquid[9–14] and spin ice.[15–17] Magnetic materials with frustrated lattice structures are good platforms to investigate those novel properties induced by geometrical frustration, where the interaction between spins cannot be simultaneously satisfied. Although a lot of work has been reported about those novel properties, the underlying mechanism needs to be further studied on more geometrically frustrated materials.

$Ni_3Sn_2$ is a transition metal compound, with two different phases at different temperature ranges.[18–20] The low temperature phase (LTP) $Ni_3Sn_2$ has a $Ni_3Sn_2$-type orthorhombic structure with the space group *oP*12/*Pnma*. Above ~780 K the compound transforms to a high temperature phase (HTP) $Ni_3Sn_2$, which has a $Ni_2In$-type hexagonal structure with the space group $P6_3/mmc$. In HTP-$Ni_3Sn_2$, Ni atoms with different coordination form the triangular lattices, which is one of the key ingredients for spin frustration that may induce quantum phenomena with exotic physical properties. Though crystal structure and phase diagram for $Ni_3Sn_2$ have been reported in the previous studies,[18–20] less work has been done to study the magnetic and transport properties.

In this work, we first report magnetic and transport properties of HTP-$Ni_3Sn_2$ single crystal. The magnetic measurements show that HTP-$Ni_3Sn_2$ is a paramagnetic compound with an obvious magnetic anisotropy. Due to the existence geometrical frustration arising from the triangular nickel lattices, the long range magnetic order is not observed. The temperature dependence of the resistivity and MR also reveal a strong contribution from the short range magnetic order. Our results suggest that the long-range magnetic order may be suppressed by the geometrical frustration in HTP-$Ni_3Sn_2$.

## 2. Experimental

Single crystals of HTP-$Ni_3Sn_2$ were first grown by the chemical vapor transport method by using iodine as a transport agent. The detailed process can be described as follows. The polycrystalline $Ni_3Sn_2$ was obtained by reacting Ni powder with Sn powder with Ni : Sn = 3 : 2 at 800 °C for 3 days. The polycrystalline powder together with iodine was sealed in a long quartz tube under vacuum. The quartz tube was then kept in a gradient furnace for 7 days with the cooler end at 1000 °C, while the hot end with the mixed powder at 1070 °C. The quartz tube naturally cooled to 800 °C in furnace, and then quenching. Single crystals of HTP-$Ni_3Sn_2$ were obtained at the cooler end. Single crystal X-ray diffraction (XRD) was used to determine crystal growth orientation (Rigaku-TTR3). The transport measurements were investigated on the Oxford Instrument TeslatronPT cryogenic system by four probe technique. The magnetic measurements were carried out using the Quantum Design 7 T Magnetic Property Measurement System.

## 3. Results and discussion

The HTP-$Ni_3Sn_2$ has a $Ni_2In$-type hexagonal structure with the $P6_3/mmc$ space group, as shown in Fig. 1(a). Ni atoms occupy two positions and form triangular lattices, which is presented in

[a]*The Anhui Key Laboratory of Condensed Matter Physics at Extreme Conditions, High Magnetic Field Laboratory, Chinese Academy of Sciences, Hefei 230031, China. E-mail: xiancong@hmfl.ac.cn*

[b]*University of Science and Technology of China, Hefei 230026, China*

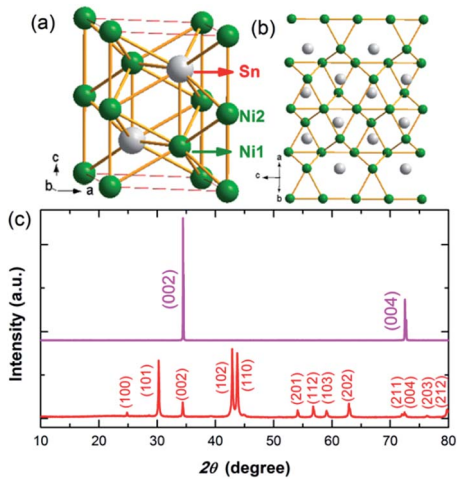


Fig. 1 (a) The crystal structure of HTP-$Ni_3Sn_2$. (b) The triangular lattices of Ni atoms. (c) The single-crystal and powder XRD patterns of HTP-$Ni_3Sn_2$.

Fig. 1(a) and (b). Two Ni2 atoms and a Ni1 atom form the triangular lattices with distorted configuration, indicating the existence of frustrated structures. The single crystal and powder XRD of HTP-$Ni_3Sn_2$ are presented in Fig. 1(c). Only $(00m)$ reflections are present in the single crystal XRD, indicating the large surface of HTP-$Ni_3Sn_2$ crystal is *ab* plane. The *c* axis lattice parameter is estimated to be 5.208 Å from the (002) peak position by using Bragg's law. In order to verify whether the sample is a single phase compound, we studied the XRD of the powder sample ground from single crystals, which is consistent with the data of the HTP-$Ni_3Sn_2$.[18] The results also indicate that the sample has a pure phase.

To investigate the magnetic properties of HTP-$Ni_3Sn_2$, magnetic susceptibility ($\chi = M/H$) measurements on a single-crystalline HTP-$Ni_3Sn_2$ was performed. Fig. 2 shows the temperature dependence of susceptibility $\chi$ at 0.1 T and the $T$ range 2 K $\leq T \leq$ 300 K for both magnetic field directions. It's obvious that the paramagnetic behaviour is presented for both directions. And the value of $\chi$ for *c* axis is larger than that of *ab* plane, indicating that the *c* axis has stronger magnetic correlations. The anisotropy ratio $\gamma = \chi_c/\chi_{ab}$ as a function of temperature is shown in the inset of Fig. 2(b). With decreasing the temperature, the $\gamma$ slowly increases at the temperature of 120–300 K and then decreases down to 2 K. In general, $\chi$ slowly increases due to the thermal fluctuation at high temperature, leading to a little change for the value of $\gamma$. Upon further decreasing temperature, $\chi$ increases sharply with the decrease of thermal fluctuation. The anisotropic magnetic structure results in the obvious difference of slope of $\chi$ for both directions. It is obvious that the slope of $\chi$ for *ab* plane is more than that for *c* axis at low temperature. Therefore, the value of $\gamma$ decreases. In the paramagnetic regime, the $\chi(T)$ curves follow the Curie–Weiss law $\chi(T) = \chi_0 + C/(T - \theta_p)$, where $\chi_0$ is a $T$-independent contribution term of the susceptibility, $C$ is the Curie constant and $\theta_p$ is the Weiss temperature. The derived

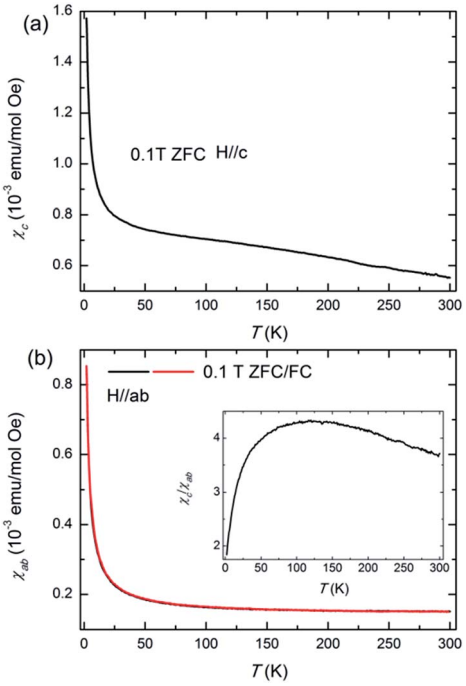


Fig. 2 The susceptibility $\chi$ for HTP-$Ni_3Sn_2$ crystal *versus* temperature $T$ for 2 K $\leq T \leq$ 300 K in the magnetic field applied (a) along the *c* axis and (b) perpendicular to the *c* axis. The inset is the temperature dependence of susceptibility anisotropy ratio $\gamma = \chi_c/\chi_{ab}$ at 0.1 T.

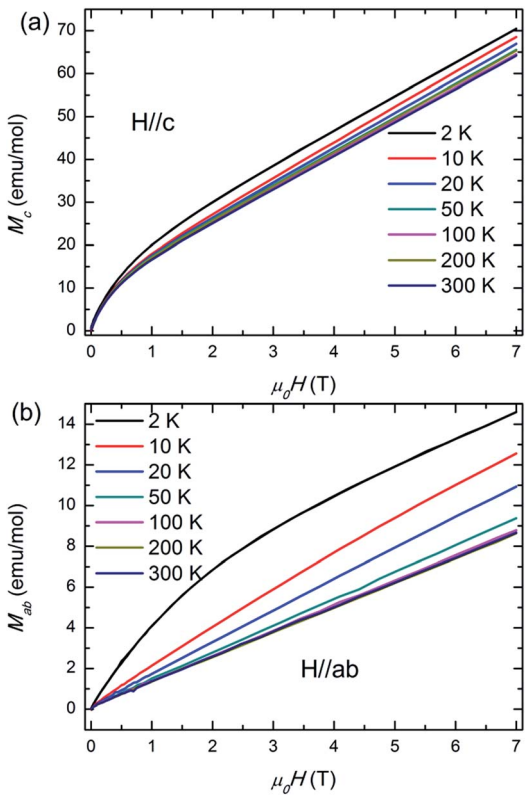


Fig. 3 Magnetization $M$ of HTP-$Ni_3Sn_2$ single crystal as a function of applied magnetic field $H$ measured at the indicated temperatures from 2 K to 300 K with the magnetic field applied (a) along the *c* axis and (b) perpendicular to the *ab* axis.

effective moments are 1.96 $\mu_B$/Ni for $H\|c$ and 0.07 $\mu_B$/Ni for $H\|ab$, indicating that the $c$ axis is the easy axis and has a stronger magnetic correlation. The effective moments for the $c$ axis is close to the theoretical value of 1.73 $\mu_B$/Ni for $S = 1/2$ $Ni^{3+}$ ions and less than the theoretical value of 2.83 $\mu_B$/Ni for high spin $S = 1$ $Ni^{2+}$ ions.[21] In addition, the obtained Curie–Weiss temperatures $\theta_p$ are −1102 K and 23 K for $H\|c$ and $H\|ab$. The large negative Weiss temperature indicates strong antiferromagnetic correlations along $c$ axis. In spite of the observed large negative Weiss temperature, the long range magnetic order is absent in $\chi(T)$ because the geometrical frustration suppress the long-range magnetic order. As we known, this situation often is observed in frustrated materials. For example, despite existence of antiferromagnetic interaction, $Pr_2Ir_2O_7$ has no long range magnetic order due to strong geometrical frustration.[22] For HTP-$Ni_3Sn_2$, the geometrical frustration in the triangular nickel lattice shown in Fig. 1 is likely a possibility to result in the absence of long range magnetic order.

Magnetization $M$ of HTP-$Ni_3Sn_2$ single crystal as a function of applied magnetic field $H$ measured at different temperatures between 2 K and 300 K for $H$ applied along the $c$ axis and perpendicular to the $ab$ axis are shown in Fig. 3(a) and (b), respectively. For the $c$ axis, the $M$ increases sharply upon the increase of field at low field (<1 T), then the $M$ increases linearly and shows no saturation at all temperatures. But for the $ab$ plane, only the behaviour of $M$ at 2 K is similar with that for $c$ axis due to the magnetic correlation is weak and suppressed with increasing the temperature. At other indicated temperatures, the $M$ increases linearly and shows no saturation. This also indicates that HTP-$Ni_3Sn_2$ has an anisotropic magnetic structure.

The temperature dependence of the electrical resistivity $\rho(T)$ down to 2 K for HTP-$Ni_3Sn_2$ single crystals is shown in Fig. 4(a). The $\rho(T)$ at zero field exhibits a metallic behaviour. At low temperature, a kondo-like increase of resistivity was observed, which is due to the scattering of conducting carriers from the magnetic atoms. But above ~80 K, the resistivity $\rho$ temperature dependence is different with the ordinary metals. For the ordinary metals, the temperature dependence of the total resistivity at high temperature is $T$-linear mainly due to electron–phonon scattering.[23,24] But for HTP-$Ni_3Sn_2$, the sublinear temperature dependence was presented at high temperature. The red sublinear lines shows the fitting results by using the formula $\rho = A + BT^n$, obtaining $n = 0.07$ at the temperature of 80–200 K ($n < 1$), which is unusual. This abnormal behaviour for resistivity is attributable to the short-range order correlations arising from the geometrical frustration, indicating the geometrical frustration is existed in this material. The similar behaviour was also observed in the frustrated compound $PdCrO_2$.[25]

Magnetic field dependence of in-plane magnetoresistance (MR) at indicated temperatures are showed in Fig. 4(b). The MR is calculated by $\Delta\rho/\rho = [\rho(H) - \rho(0)]/\rho(0)$. The positive MR is presented under the magnetic field up to 9 T at different temperatures. At 2 K and 9 T, the value of MR reaches the

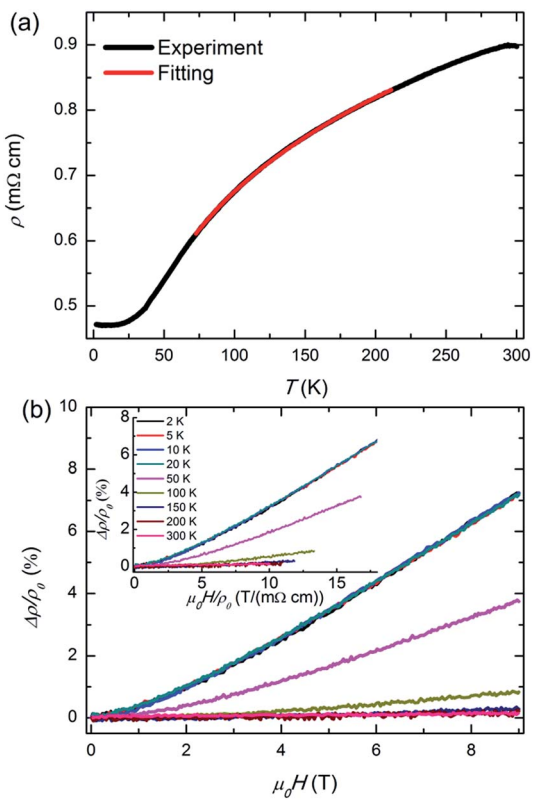


Fig. 4 (a) Temperature dependence of resistivity $\rho$ at temperature ranging from 2 K to 300 K. (b) Magnetoresistance for HTP-$Ni_3Sn_2$ at various temperatures. Inset: corresponding $\Delta\rho/\rho(0)$ *vs.* $H/\rho(0)$.

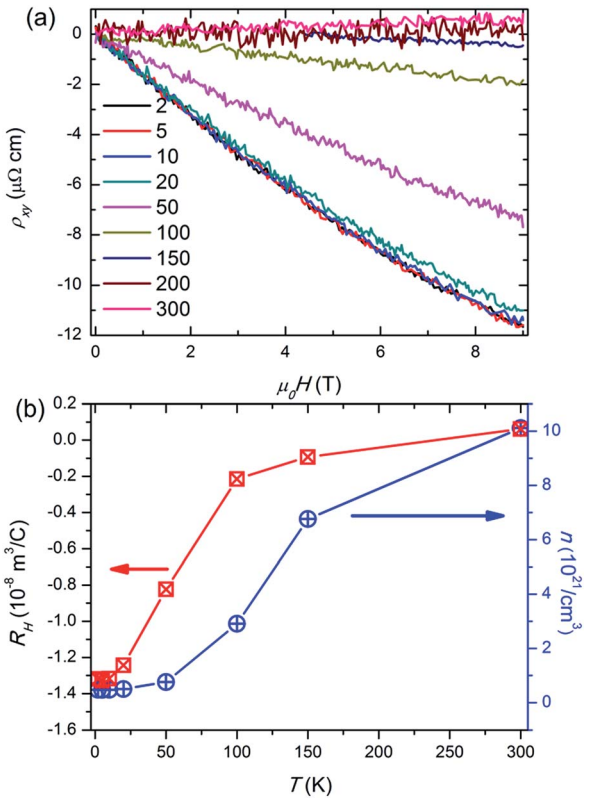


Fig. 5 (a) The magnetic field dependence of Hall resistivity $\rho_{xy}$ at various temperatures. The magnetic field is along $c$ axis and current is in $ab$ plane. (b) The Hall coefficient $R_H$ and carrier concentrations $n$ for HTP-$Ni_3Sn_2$ from 2 K to 300 K.

maximum value, which is ~7%. With increasing temperature, the MR decreases and then tends to the zero. According to the Kohler's Rule,[26] the MR *versus* $H/\rho(0)$ have a universal function $\Delta\rho/\rho(0) = f(H/\rho(0))$ for the metals at all temperatures and fields. Here, we also analysed the data of MR by the Kohler's Rule, as shown in the inset of Fig. 4(b). It's obvious that the MR deviates from the Kohler's law at $T > 50$ K. This may be due to the change of contribution from magnetic scattering upon the change of temperature. Based on the above results of transport, we would conclude that the magnetic correlations have an important influence on the transport properties of HTP-$Ni_3Sn_2$.

To quantify the electrical transport properties under applied magnetic field, the field dependence of Hall resistivity $\rho_{xy}$ of HTP-$Ni_3Sn_2$ is investigated under $H\|c$ at different temperatures, as shown in Fig. 5(a). The $\rho_{xy}$ shows nearly linear dependence to the applied field in the whole temperature range, indicating that $\rho_{xy}$ is derived from the ordinary Hall effect. And the $\rho_{xy}$ decreases with the increase of $H$. This suggests that the electron-type carrier in HTP-$Ni_3Sn_2$ is dominant. The Hall coefficient ($R_H$) and carrier concentrations ($n = -1/(eR_H)$) were presented in Fig. 5(b). The normal Hall coefficient $R_H$ reaches the maximum of $\sim -1.3 \times 10^{-8}$ m$^3$ C$^{-1}$ at 2 K. which is an order of magnitude less than that in $Fe_3Sn_2$.[27] The carrier concentrations $n$ varies from the minimal value $0.5 \times 10^{21}$ cm$^{-3}$ at 2 K to $1.0 \times 10^{22}$ cm$^{-3}$ at 300 K, which is in the range of typical metal.

## 4. Conclusions

In summary, we synthesized single crystals of HTP-$Ni_3Sn_2$ by using chemical vapor transport method and characterized their magnetic and transport properties. The anisotropic magnetic properties were presented on HTP-$Ni_3Sn_2$. Due to the geometrical frustration arising from the triangular nickel lattice, the long range magnetic order is absent. In addition, the sublinear temperature dependence of the resistivity was presented and the MR deviates from the Kohler's law. The detailed analysis proposes that the magnetic correlations play an important role on the transport properties of HTP-$Ni_3Sn_2$.

## Conflicts of interest

There are no conflicts to declare.

## Acknowledgements

This work is supported by the Ministry of Science and Technology of China (National Key Research and Development Program No. 2016YFA0300404), and the National Natural Science Foundation of China (Grant No. U1432138, 11474288, 11604344, 11574322, 21503233, 11574317).

## References

1 L. Balents, *Nature*, 2010, **464**, 199–208.
2 V. Fritsch, J. Hemberger, N. Büttgen, *et al.*, *Phys. Rev. Lett.*, 2004, **92**, 116401.
3 G. Chen, L. Balents and A. P. Schnyder, *Phys. Rev. Lett.*, 2009, **102**, 096406.
4 R. Moessner and A. P. Ramirez, *Phys. Today*, 2006, **59**, 24.
5 Y. Taguchi, Y. Oohara, H. Yoshizawa, N. Nagaosa and Y. Tokura, *Science*, 2001, **291**, 2573–2576.
6 Y. Taguchi, T. Sasaki, S. Awaji, *et al.*, *Phys. Rev. Lett.*, 2003, **90**, 257202.
7 C. Sürgers, G. Fischer, P. Winkel and H. V. Löhneysen, *Nat. Commun.*, 2014, **5**, 3400.
8 S. Nakatsuji, N. Kiyohara and T. Higo, *Nature*, 2015, **527**, 212–215.
9 R. Moessner and J. T. Chalker, *Phys. Rev. Lett.*, 1998, **80**, 2929–2932.
10 R. Moessner and A. P. Ramirez, *Phys. Today*, 2006, **59**, 24.
11 B. G. Levi, *Phys. Today*, 2007, **60**, 16.
12 T. Imai and Y. S. Lee, *Phys. Today*, 2016, **69**, 30.
13 M. R. Norman, *Rev. Mod. Phys.*, 2016, **88**, 041002.
14 L. Savary and L. Balents, *Rep. Prog. Phys.*, 2017, **80**, 016502.
15 C. Castelnovo, R. Moessner and S. L. Sondhi, *Nature*, 2008, **451**, 42–45.
16 S. T. Bramwell, S. R. Giblin, S. Calder, R. Aldus, D. Prabhakaran and T. Fennell, *Nature*, 2009, **461**, 956–959.
17 H. R. Molavian, M. J. P. Gingras and B. Canals, *Phys. Rev. Lett.*, 2007, **98**, 157204.
18 G. F. Zhou, L. M. Di and H. Bakker, *J. Appl. Phys.*, 1993, **73**, 1521–1527.
19 C. Schmetterer, H. Flandorfer, K. W.Richter, *et al.*, *Intermetallics*, 2007, **15**, 869–884.
20 A. Leineweber, E. J. Mittemeijer, M. Knapp, *et al.*, *Philos. Mag.*, 2007, **87**, 1821–1844.
21 N. W. Ashcroft and N. D. Mermin, *Solid state physics*, 1976, ch. 31, p. 658.
22 Y. Machida, S. Nakatsuji, Y. Maeno, T. Tayama, T. Sakakibara and S. Onoda, *Phys. Rev. Lett.*, 2007, **98**, 057203.
23 T. Kasuya, *Prog. Theor. Phys.*, 1956, **16**, 58.
24 K. Mori and K. Sato, *J. Phys. Soc. Jpn.*, 1980, **49**, 246.
25 H. Takatsu, H. Yoshizawa, S. Yonezawa and Y. Maeno, *Phys. Rev. B: Condens. Matter Mater. Phys.*, 2009, **79**, 104424.
26 L. Forr, K. Biljakovi, J. R. Cooper and K. Bechgaard, *Phys. Rev. B: Condens. Matter Mater. Phys.*, 1984, **29**, 2839–2842.
27 Q. Wang, S. Sun, X. Zhang, F. Pang and H. Lei, *Phys. Rev. B: Condens. Matter Mater. Phys.*, 2016, **94**, 075135.